

Fast-Neutron Scattering from Germanium*

D. LISTER† AND A. B. SMITH

Argonne National Laboratory, Argonne, Illinois 60439

(Received 27 January 1969)

Elastic and inelastic neutron scattering cross sections of natural germanium were measured in the incident neutron energy range 0.3–1.5 MeV with incident energy resolutions of ~ 20 keV. Neutron-velocity and γ -ray spectroscopic methods were employed to resolve the scattering to individual low-lying states. The results were interpreted in terms of the optical model and the statistical compound-nucleus model including effects due to fluctuations and correlations of resonance widths. Measured cross sections for inelastic scattering to a number of excited states in even Ge isotopes were reasonably well described by the statistical model of Hauser and Feshbach without corrections for width fluctuations and correlations.

I. INTRODUCTION

NEUTRON-NUCLEUS interactions in the medium- and heavy-mass regions are dominated by “shape-elastic” scattering and compound-nucleus (CN) processes for incident energies up to a few MeV. The shape-elastic component has been successfully described over a wide range of masses and energies in terms of the optical model.¹ Computation of average CN cross sections has often been based on the statistical CN model of Wolfenstein² and Hauser and Feshbach.³ In recent years, the latter calculations have been modified to include corrections arising from the consideration of fluctuations and correlations in the reduced widths of CN resonances.⁴ This modified CN model contains a number of approximations and it is of interest to examine its validity by detailed comparison with experimental results from a number of nuclear systems. The purpose of the present work was to experimentally study the interaction of neutrons with germanium in the incident neutron energy range 0.3–1.5 MeV in order to contribute to the understanding of CN processes in medium-weight nuclei.

Elemental germanium consists of the isotopes 70, 72, 73, 74, and 76, the low-energy level schemes of which have been reasonably well established.⁵ Neutron interactions with germanium have been studied qualitatively^{6,7} and quantitatively^{8–11} at several incident energies. Cox has measured neutron elastic scattering cross sections in the region 0.7–1.2 MeV with good energy resolution.¹² Barry has deduced relative inelastic

scattering cross sections from γ -ray yields in $\text{Ge}(n, n'\gamma)$ processes at a number of bombarding energies between 0.5 and 2.5 MeV.¹³ Neutron inelastic scattering cross sections have also been reported by Chung *et al.*¹⁴ Measured neutron total cross sections of germanium have been compiled in graphic¹⁵ and tabular¹⁶ forms. Further, the good energy resolution (≈ 2 keV) recently employed in total cross-section measurements by Whalen and Meadows¹⁷ has revealed pronounced fluctuations in the total cross sections of natural germanium throughout the incident energy range of 0.10–0.65 MeV. A number of these previous studies have compared experiment with calculation but none has provided the detailed, direct, and internally consistent experimental understanding of (n, n) and (n, n') processes over an appreciable incident neutron energy range needed for a critical assay of theoretical concepts. It was an objective of this work to provide such information.

II. PROCEDURE

A. Neutron Time-of-Flight Measurements

Differential elastic and inelastic neutron scattering cross sections of germanium were measured by means of the fast neutron time-of-flight technique¹⁸ over the incident neutron energy range from 0.3 to 1.5 MeV. The apparatus, the experimental procedure, and the information processing have been extensively described elsewhere¹⁹ and are only outlined below.

A pulsed 3-MeV Van de Graaff accelerator was used together with a magnetic bunching system of the Mobley type²⁰ to produce intense nanosecond ion bursts

* Work supported by the U.S. Atomic Energy Commission.
† Present address: Princeton Gamma-Tech., P.O. Box 641, Princeton, N.J. 08540.

¹ P. E. Hodgson, *The Optical Model of Elastic Scattering* (Oxford University Press, London, 1963).

² L. Wolfenstein, *Phys. Rev.* **82**, 690 (1951).

³ W. Hauser and H. Feshbach, *Phys. Rev.* **87**, 366 (1952).

⁴ P. A. Moldauer, *Rev. Mod. Phys.* **36**, 1079 (1964).

⁵ *Nuclear Data Sheets*, compiled by K. Way *et al.* (Printing and Publishing Office, National Academy of Sciences—National Research Council, Washington, D.C., 1966).

⁶ S. S. Malik *et al.*, *Bull. Am. Phys. Soc.* **4**, 259 (1959).

⁷ C. Chasman *et al.*, *Nucl. Instr. Methods* **37**, 1 (1965).

⁸ R. M. Sinclair, *Phys. Rev.* **107**, 1306 (1957).

⁹ K. Nishimura, *J. Phys. Soc. Japan* **16**, 355 (1961).

¹⁰ D. Kent *et al.*, *Phys. Rev.* **125**, 331 (1962).

¹¹ R. Becker *et al.*, *Nucl. Phys.* **89**, 154 (1966).

¹² S. A. Cox (private communication).

¹³ J. F. Barry, in *Nuclear Data for Reactors* (International Atomic Energy Agency, Vienna, 1967), Vol. 1, p. 365; also, J. F. Barry (private communication).

¹⁴ D. Chung *et al.*, *Bull. Am. Phys. Soc.* **13**, 601 (1968).

¹⁵ D. J. Hughes and R. Schwartz, *Brookhaven National Laboratory Report No. 325* (U.S. Government Printing Office, Washington, D.C., 1958), 2nd ed.

¹⁶ R. J. Howerton, University of California Radiation Laboratory Report No. UCRL-5226, Part 1, Vol. II, 1958 (unpublished).

¹⁷ J. Whalen and J. Meadows (private communication).

¹⁸ L. Cranberg and J. S. Levin, *Phys. Rev.* **103**, 343 (1956); see also, A. B. Smith, in *Nuclear Research with Low Energy Accelerators*, edited by J. B. Marion and D. M. Van Patter (Academic Press Inc., New York, 1967), pp. 359–387.

¹⁹ A. Smith *et al.*, *Nucl. Instr. Methods* **50**, 277 (1967).

²⁰ R. C. Mobley, *Phys. Rev.* **88**, 360 (1952).

at a neutron-producing target. The ${}^7\text{Li}(p, n){}^7\text{Be}$ reaction was the primary neutron source. Scattering samples of natural germanium in the form of 2.0-cm-diam \times 2.0-cm-high right circular cylinders were positioned approximately 11 cm from the neutron source at 0° with respect to the incident proton beam. The sample axes were oriented perpendicular to the horizontal scattering plane. The neutron detection system consisted of a multiangle array of eight well-shielded liquid organic scintillators. The scintillators viewed the sample through suitable collimators. In this study the observed laboratory scattering angles were approximately 28° , 39° , 53° , 69° , 84° , 114° , 129° , and 154° . Flight paths were ≈ 200 cm and measurements were made concurrently at the eight scattering angles. The detectors were sensitive to neutrons of ≥ 200 -keV energy and the scattered neutron time resolution was ≈ 1.5 nsec/m. The incident neutron energy resolution was ≈ 20 keV and angular distributions were determined at incident energy intervals of 20 keV or less. All time-of-flight measurements were made relative to the established differential elastic scattering cross sections of carbon²¹ and corrected for incident beam attenuation, angular resolution, and multiple scattering effects.¹⁹ Scattered neutron flight times were determined by means of a standard time-delay system and verified by the observation of inelastic scattering from well-known states,⁵ particularly the 845-keV state in ${}^{56}\text{Fe}$. A representative scattered neutron velocity spectrum is shown in Fig. 1.

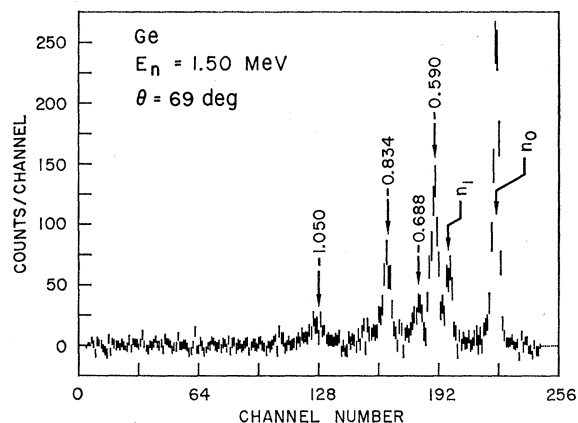


FIG. 1. Illustrative time-of-flight spectrum obtained for the scattering of 1.50-MeV neutrons from natural Ge through an angle of 69° . Neutron groups scattered from various states are indicated. Backgrounds have been subtracted and bar lengths denote statistical errors. Peaks marked n_0 and n_1 indicate elastically scattered first and second neutron ${}^7\text{Li}(p, n){}^7\text{Be}$ source groups, respectively. Inelastically scattered groups are denoted by their observed Q values in MeV. Flight path was ≈ 200 cm, time per channel ≈ 1.1 nsec.

²¹ A. Langsdorf *et al.*, Argonne National Laboratory Report No. ANL-5567, 1961 (unpublished); see also R. Lane *et al.*, *Ann. Phys.* (N.Y.) **12**, 135 (1961).

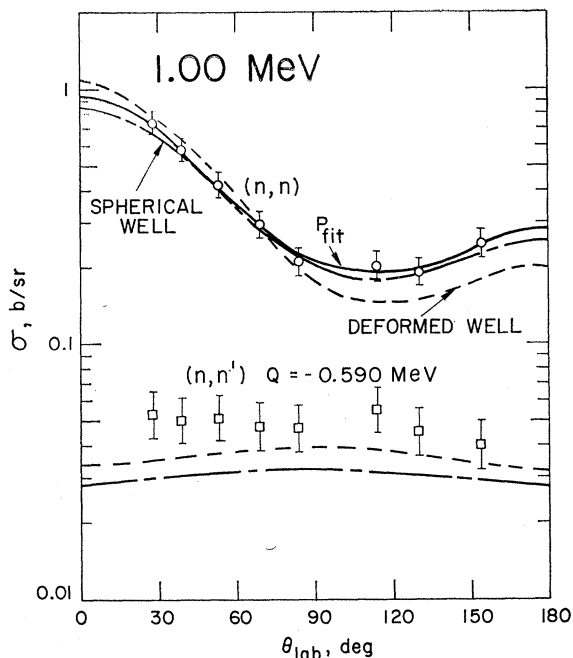


FIG. 2. Differential cross sections for elastic and inelastic neutron scattering from natural germanium at an incident energy of 1.0 MeV. Measured values are shown as open circles and squares; the error bars denote estimated uncertainties. The solid curve is the result of a $L=4$ least-square fit of Eq. (1) to the measured distribution. The results of spherical optical-model and Hauser-Feshbach calculations for the element are indicated by dotted dashed curves. Dashed curves show the results of deformed coupled-channel calculations for the isotope ${}^{74}\text{Ge}$ adjusted for isotopic abundance. The observed Q value is indicated.

The measured elastic scattering angular distributions were expressed as an expansion in Legendre polynomials of the form

$$\sigma(\theta_{\text{lab}}) = (\sigma_{\text{el}}/4\pi) \left[1 + \sum_{i=1}^L \omega_i P_i(\cos\theta_{\text{lab}}) \right], \quad (1)$$

where θ_{lab} is the laboratory scattering angle, P_i is the i th order Legendre polynomial, and $\sigma(\theta_{\text{lab}})$ is the laboratory differential cross section. The parameters σ_{el} (elastic cross section) and ω_i were obtained by least squares fitting Eq. (1) to the measured differential values. The parametrization of Eq. (1) concisely described the experimental results, permitted ready comparison of measurements made at varying angles, and was useful in the interpretation of the data. It was found that the ω_i were significantly nonzero only for $i \leq 4$ and thus the sum of Eq. (1) was terminated at $L=4$. The description of experimental results provided by Eq. (1) was judged good as illustrated by the comparisons of Fig. 2. It should be pointed out that angular distributions calculated from Eq. (1) and the experimentally derived parameters may be unreliable outside of the measured angular range, particularly at extreme back angles.

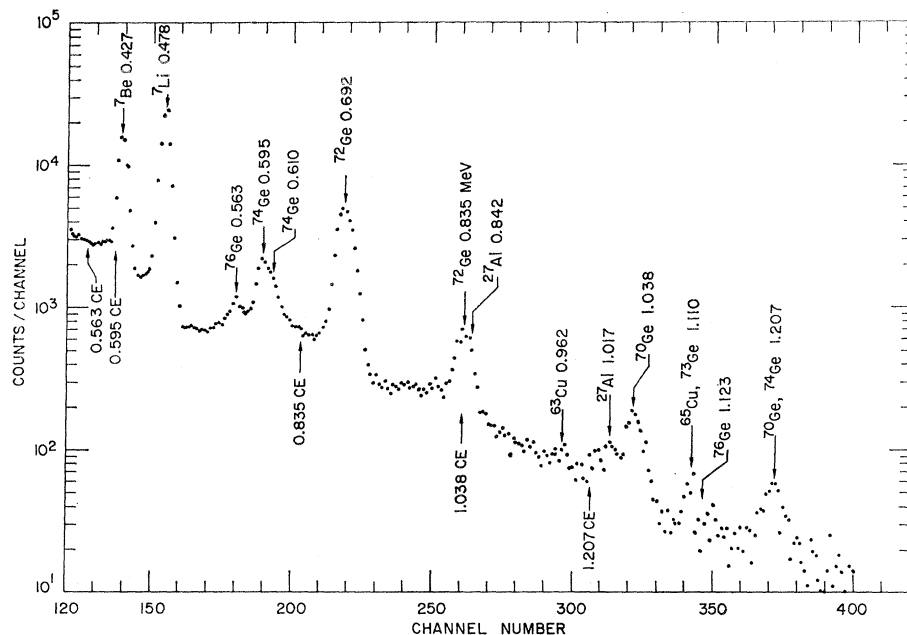


FIG. 3. Spectrum resulting from the response of the Ge(Li) detector to bombardment by 1.49-MeV neutrons. Observed transitions are identified and correlated with known γ -ray transitions in Ge, in nearby structural material, and in the ${}^7\text{Li}(p, n){}^7\text{Be}$ neutron source. The positions of some of the corresponding Compton edges (CE) are indicated. The differential energy scale is approximately 3.3 keV per channel.

The integrated cross sections for the inelastic neutron excitation of various states were obtained from a simple average of the measured differential cross-section values. This was judged a reasonable procedure as the uncertainties at the individual data points were appreciable and measured inelastic angular distributions were essentially isotropic (see Fig. 2, for example). Some of the inelastic scattering data at the smaller scattering angles ($\lesssim 35^\circ$) were omitted because of uncertainties arising from high backgrounds and from the "tails" of large elastic scattering peaks.

The sensitivity of the detectors was a rapidly varying function of neutron energy in the low-energy region. It was felt that the results for scattered neutrons having energies less than ≈ 300 keV were uncertain and therefore were not used. The resolutions, backgrounds, and counting statistics were such that the sensitivity of the system was $\lesssim 4$ mb sr^{-1} under favorable conditions.

B. γ -Ray Studies

Excitation functions for inelastic neutron scattering from germanium were deduced from the self-detected decay γ -ray spectra observed in a Ge(Li) detector bombarded by monoenergetic neutrons from the ${}^7\text{Li}(p, n){}^7\text{Be}$ reaction. Measurements were made at 10-keV intervals in the incident neutron energy range 0.59–1.49 MeV. The neutron-beam energy spread was approximately 15 keV. A cooled planar Ge(Li) detector of cylindrical shape having a stated sensitive volume of 5.7 cm^3 was positioned at 0° with respect to the incident proton beam at a distance of 115 cm from the neutron source.²² The neutron beam was confined to a 6.03-cm-

diam circular area at the detector by means of a 64-cm-long brass-lead collimator.

The neutron flux at the position of the Ge(Li) detector chamber was measured relative to the total n - p cross section²³ by means of a low-mass hydrogen-filled proportional counter of well-defined active volume.²⁴ Pulse-shape discrimination was employed to eliminate γ -ray backgrounds in the hydrogen recoil spectra. In these measurements, the Ge(Li) detector was replaced by the proportional counter; the experimental geometry otherwise remained identical. All runs were accompanied by background measurements made with the aperture of the collimator blocked with a 45-cm-long solid brass bar. The relative neutron source intensity was monitored with a "long counter"²⁵ placed at 30° with respect to the proton-beam direction. Neutron monitor counts were compared to the integrated proton current to verify target stability.

Electronic pulses from the Ge(Li) detector were amplified and shaped in a charge-sensitive preamplifier and fed into a pole-zero compensated amplifier having 1.2- μsec rise and fall time constants. The output of the amplifier was fed into a 512-channel analyzer. Neutron radiation damage had reduced the Ge(Li) detector resolution to $\approx 2\%$, FWHM (full width at half-maximum). This resolution was adequate to resolve most of the γ rays. A typical background-subtracted spectrum obtained with this detector is shown in Fig. 3. The

²³ J. L. Gammel, in *Fast Neutron Physics*, edited by J. B. Marion and J. L. Fowler (Wiley-Interscience, Inc., New York, 1963), Part 2, pp. 2185–2226.

²⁴ E. F. Bennett, *Nucl. Sci. Eng.* **27**, 16 (1967).

²² The Ge(Li) detector was prepared by H. Mann, Argonne National Laboratory.

²⁵ W. D. Allen, in *Fast Neutron Physics*, edited by J. B. Marion and J. L. Fowler (Wiley-Interscience, Inc., New York, 1961), Part 1, pp. 361–386.

particularly intense 0.692-MeV line in the figure was because of the $0^+ \rightarrow 0^+$ transition in ^{72}Ge which proceeds almost entirely by electron conversion.²⁶ The residual background present in channels representing energies greater than the bombarding energy was attributed to fast-neutron capture events. Calculation of the γ -ray energies associated with the full-energy peaks was based on the assumption that the energy was

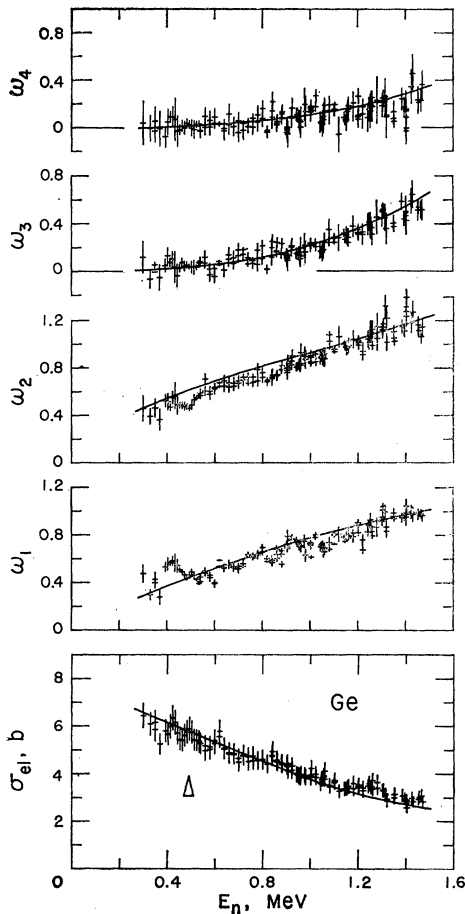


FIG. 4. Measured differential elastic neutron scattering cross sections of elemental germanium (crosses) expressed in the form of Eq. (1). The solid curves indicate the results of calculation as described in the text.

a linear function of the pulse height. The linearity of the electronics system was verified using a precision pulse generator. The 0.4776-MeV line²⁷ of ^7Li excited in the target by the (p, p') reaction and the 0.8347-MeV line⁸ of ^{72}Ge served to calibrate the system. The uncertainties in the measured energies were estimated to be ± 3 keV for full-energy peaks corresponding to energies < 1 MeV increasing to ± 6 keV for energies greater than 1 MeV.

²⁶ J. J. Kraushaar *et al.*, Phys. Rev. **101**, 139 (1956).

²⁷ W. Black and R. Heath, Nucl. Phys. **A90**, 650 (1967).

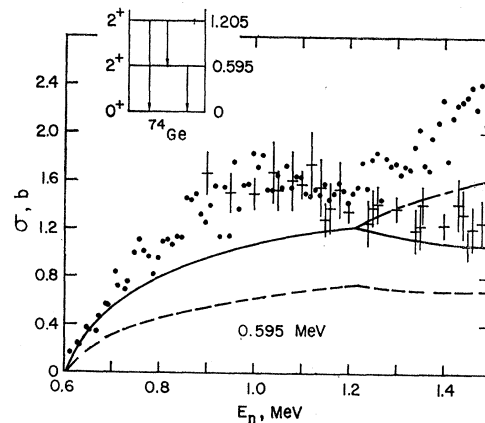


FIG. 5. Isotopic inelastic scattering cross sections of ^{74}Ge . The $(n, n'\gamma)$ data (solid circles) are normalized to the time-of-flight results (crosses) as described in the text. The solid curves were obtained from Hauser-Feshbach calculations using the illustrated level scheme. The long-short dashed curve is the calculated result inclusive of the cascade from the 1.205-MeV state. The short-dashed curve indicates results of calculations incorporating width fluctuation and correction terms with the statistical parameter $Q_\alpha=0$ [see Eq. (3)]. Vertical bars indicate the estimated experimental error in the time-of-flight measurements.

The photopeak efficiency curve for the detector was determined with the aid of a number of calibrated commercial γ -ray sources²⁸ ranging in energy from 0.087 to 1.333 MeV. The source strength was specified by the supplier to within $\pm 5\%$. An independent measurement at this laboratory²⁹ agreed with the supplier's figures to within 10% in the region between 0.662 and 1.28 MeV. Relative yield curves for the various transitions were obtained from the full-energy peak counting rate per unit incident neutron flux. Spectral backgrounds were visually estimated from the plotted spectra with

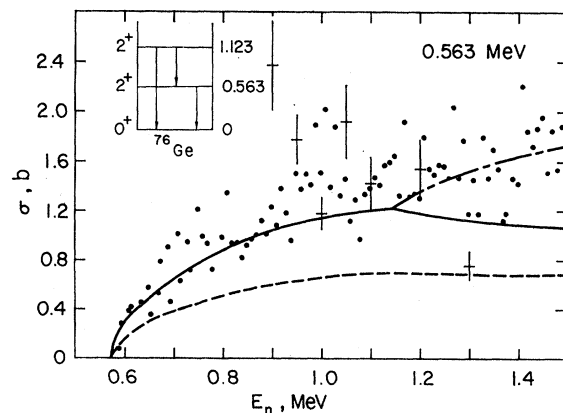


FIG. 6. Isotopic cross sections for inelastic neutron scattering from ^{76}Ge . The format is the same as that of Fig. 5. A 70% probability for the unresolved cascade was assumed in the calculation of the dashed curve.

²⁸ Obtained from Tracerlab Inc., Waltham, Mass.

²⁹ D. W. Engelkemeir (private communication).

careful consideration given to the contributions of Compton scattering.

An attempt was made to compute absolute neutron inelastic scattering cross sections from relative peak yields, measured photopeak efficiency, branching ratios, internal conversion coefficients,³⁰ and the active volume, density, and isotopic composition of the Ge(Li) detector. Corrections for the effects of neutron attenuation and scattering and for the presence of the second neutron group from the source were applied. The small effect of cascade coincidence-summing in the detector was neglected and a number of simplifying assumptions were made in estimating the response of the detector to sources distributed throughout the bulk of the material. Comparison of the resulting cross sections with those derived from the neutron time-of-flight work indicated a large discrepancy (approximately a factor of 3) between the values for the excitation of the 0+, 0.692-MeV state in ⁷²Ge determined with the two methods. Of the prominently excited states observed, only this one decayed almost entirely by internal conversion processes. As the range of the conversion electrons was short compared to the Ge(Li) crystal dimensions and they were counted with 100% efficiency, their detection was used to indicate the detector active volume. Comparison of the results of the efficiency calibrations and the values obtained from Monte Carlo calculations of γ -ray transport in bulk germanium³¹ further indicated that the actual active volume of the detector was approximately one-third the volume determined by the copper staining technique in fabrication.

In view of the above uncertainties in the calculation of inelastic cross sections directly from the Ge(Li) data, the following normalization procedures were employed. The relative cross section for the excitation of the 0.595-MeV state in ⁷⁴Ge as determined from γ -emission studies was normalized to the time-of-flight result in the incident energy range 1.0–1.2 MeV. The energy dependence of the sensitivity of the Ge(Li) detector for γ rays, calculated as outlined above, was then used to determine the γ -ray transition rates of other states relative to that of the 0.595-MeV state in ⁷⁴Ge. The excitation function of the 0+ \rightarrow 0+, 0.692-MeV transition in ⁷²Ge was independently normalized to the respective time-of-flight result.

C. Analytical Procedure

The neutron elastic scattering results were analyzed in the framework of the optical model. A static, local, and spherical potential well was used having a Wood-Saxon real part, a derivative imaginary part, and a real

Thomas spin-orbit term of the following form¹;

$$V(r) = -\{V_r f(r) + V_i g(r) + V_{so}[\hbar/(m_\pi c)]^2 r^{-1} |df(r)/dr| \mathbf{1} \cdot \boldsymbol{\delta}\},$$

$$f(r) = \{1 + \exp[(r-R)/a]\}^{-1}, \quad (2)$$

$$g(r) = 4 \exp[(r-R')/b] \{1 + \exp[(r-R')/b]\}^{-2},$$

where V_r is the real-well depth, V_i is the imaginary-well depth, V_{so} is the spin-orbit well depth, R is the real-well radius, a is the real-well diffuseness, R' is the imaginary-well depth, and b is the imaginary-well diffuseness. The parameters of Eq. (2) were assumed level- and energy-independent and, except for R and R' , isotope-independent. All spherical well calculations were carried out with the ABACUS-NEARREX computer code.³² This code offered an option of CN statistical calculations with and without "corrections" for width fluctuations and correlations. In the corrected form, the compound-nucleus transmission coefficient T_α is replaced by $\langle\theta_\alpha\rangle$, where⁴

$$\langle\theta_\alpha\rangle = T_\alpha + (1/Q_\alpha)[1 - (1 - Q_\alpha T_\alpha)^{1/2}]^2. \quad (3)$$

Q_α is a statistical parameter with values $0 \leq Q_\alpha \leq 1$. Its magnitude is expected to be near zero for the present cases. Evidently, $\langle\theta_\alpha\rangle \rightarrow T_\alpha$ when either $T_\alpha \rightarrow 0$ or $Q_\alpha \rightarrow 0$ and, in the many-channel limit, the calculation reduces to the method of Wolfenstein² and Hauser and Feshbach.³ With the exception of V_{so} , the parameters were varied to obtain a "best" fit to the experimental elastic scattering and total cross sections. The judgment of "best" was based upon a subjective graphical comparison of calculated and measured quantities. The "best" well parameters were then used to calculate the excitation cross sections for the various inelastic scattering processes based initially on the statistical CN theory of Hauser and Feshbach and, secondly, the CN model inclusive of reduced width fluctuations and correlations.

III. RESULTS

A. Elastic Neutron Scattering

Values of the elastic scattering parameters, σ_{el} , $\omega_1, \dots, \omega_4$, were derived, using the method outlined above from several separate series of measurements carried out with slightly varying experimental conditions.³³ The final results were smoothed by averaging over 10-keV intervals. This averaging interval was consistent with the experimental incident energy resolution and the preservation of energy-dependent fluctuations in the scattering parameters. The results are

³² E. Auerbach, ABACUS-II, Brookhaven National Laboratory Report No. BNL-6562, 1962 (unpublished); P. Moldauer *et al.*, NEARREX, Argonne National Laboratory Report No. ANL-6978, 1964 (unpublished).

³³ Numerical values for all measured cross sections reported herein have been transmitted to the National Neutron Cross Section Center (NNCSC), Brookhaven National Laboratory.

³⁰ M. E. Rose, *Internal Conversion Coefficients* (North-Holland Publishing Co., Amsterdam, 1958).

³¹ W. J. Snow, Argonne National Laboratory Report No. ANL-7314, 1967 (unpublished).

shown in Fig. 4. An error of $\pm 8\%$ has been assigned to the quantity σ_{e1} inclusive of statistical errors, curve-fitting errors, and the $\pm 5\%$ uncertainty in the "standard" cross section of carbon. The indicated error bars for the ω coefficients represent the "goodness of fit" of Eq. (1) to the experimentally determined differential cross sections and do not necessarily reflect all the experimental uncertainties.

The optical-model calculational procedures above, yielded the "best" set of well parameters: $V_r=46$ MeV,

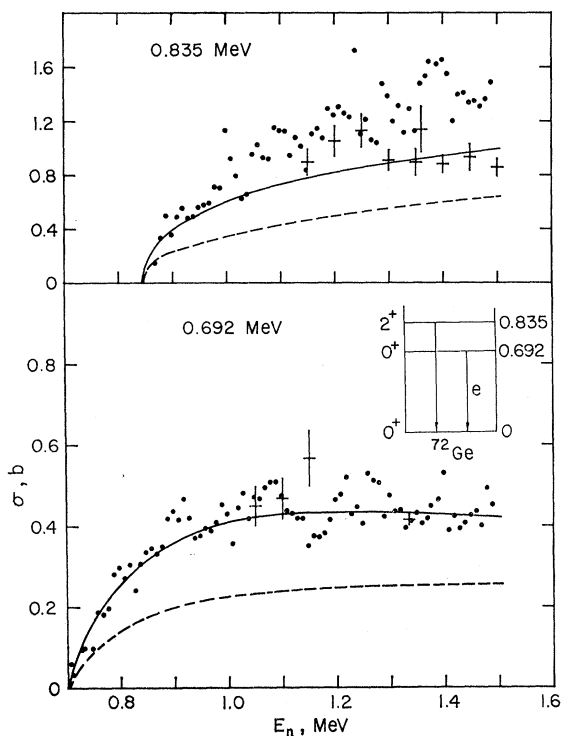


FIG. 7. Isotopic cross sections for inelastic neutron scattering from the 0.692- and 0.835-MeV states of ^{72}Ge . Measured points and calculated curves use the same notation as in Fig. 5. The normalization and uncertainties of the data are discussed in the text.

$V_i=8$ MeV, $V_{so}=7$ MeV, $a=0.65$ F, $b=0.50$ F, $R=R'=(1.16A^{1/3}+0.6)$ F, where A is the nuclear mass number. These potential parameters were similar to those used by other authors in the analysis of low-energy neutron data.^{34,35} The calculated results were relatively insensitive to differences between R and R' of 1 F or less. The results of elastic scattering calculations (inclusive of compound-elastic) contributions using the above "best" set of parameters are indicated by the solid curves of Fig. 4. The agreement with an energy average of the experimental results was accept-

³⁴ P. A. Moldauer, Nucl. Phys. **47**, 65 (1963).

³⁵ F. Perey and B. Buck, Nucl. Phys. **32**, 353 (1962).

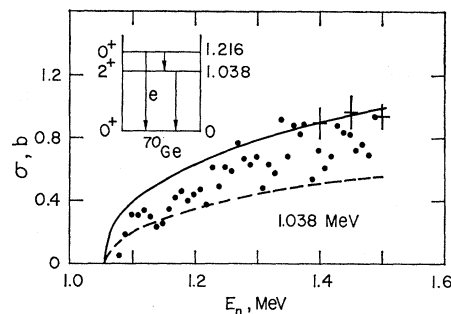


FIG. 8. Isotopic cross sections for the excitation of the 1.038-MeV state in ^{70}Ge . Notation is as for Fig. 5.

able both in the form of the Legendre expansions of Fig. 4 and for angular distributions measured at individual incident energies.

B. Inelastic Neutron Scattering

The energies of excited states observed by inelastic scattering in the present time-of-flight and γ -ray work are summarized in Table I. The results obtained from the two methods were in reasonable agreement. The energies determined from the γ -ray measurements were more precise than those obtained from the time-of-flight work and were accepted as the best values from the present work. Generally, the results of the present work were consistent with previously reported structure in the isotopes of germanium.⁵ None of the observed quantities could be exclusively attributed to the minority odd isotope ^{73}Ge . Some of the time-of-flight spectra showed neutron groups corresponding to the inelastic excitation of states in the region of 0.48–0.51 MeV. These observed groups were, within the experimental uncertainties, attributable to neutrons from the second group of the $^7\text{Li}(p, n)^7\text{Be}$ source reaction elastically scattered from the sample.

All of the measured inelastic cross sections were converted to isotopic values assuming that the natural germanium scattering sample and the Ge(Li) detector had the following isotopic composition: 20.5% ^{70}Ge , 27.4% ^{72}Ge , 7.8% ^{73}Ge , 36.5% ^{74}Ge , and 7.8% ^{76}Ge ; and

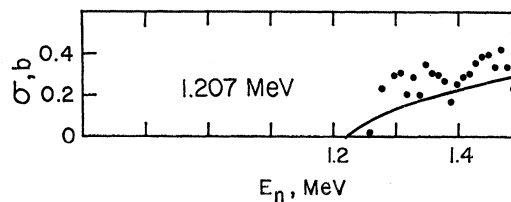


FIG. 9. Cross sections for the composite of unresolved 1.205- and 1.216-MeV transitions in ^{70}Ge and ^{74}Ge , respectively. The derivation of this average cross section is discussed in the text. The solid curve represents the results of the unmodified statistical CN calculation.

TABLE I. Observed energies of states in germanium excited by inelastic neutron scattering.

Isotope	Spin ^a	Parity ^a	Excitation ^a energy (keV)	Observed ^b transition energy (keV)	Observed ^c reaction <i>Q</i> values (keV)
⁷⁶ Ge	2	+	563	563+3	-560±10
⁷⁴ Ge	2	+	596	595±3	-590±10
⁷² Ge	0	+	690	692±3	-688±10
⁷² Ge	2	+	834.7	835 ^d	-834±5
⁷⁰ Ge	2	+	1040	1038±6	-1050±10
⁷⁴ Ge	2	+	1205	1207±6	-1228±15
⁷⁰ Ge	0	+	1216		

^a Based upon the previously reported structure as summarized in Ref. 5.
^b γ -ray transition energies as determined from the present Ge(Li) detector results.

^c Reaction *Q* values as determined from the present time-of-flight measurements.

^d Used as calibration point.

that the observed inelastic cross sections were associated with specific isotopes as indicated in Table I. The resulting measured isotopic cross sections for the excitation of each of the observed states are shown in Figs. 5-9. The measured inelastic neutron scattering angular distributions were essentially isotropic as illustrated in Fig. 2. The time-of-flight results are indicated in Figs. 5-8 by crosses, the vertical bars of which represent subjective estimates of error. If more than one measure-

ment was available at a given energy, the results were averaged.

In Figs. 5-9, the results of inelastic γ -ray measurements are indicated by solid data points. The errors in the relative cross sections associated with the intense full energy peaks were estimated to be $\pm 10\%$ and became somewhat larger for weaker transitions and for those with uncertain background contributions. Further uncertainties were associated with the normalization

TABLE II. Transition parameters and relative detection efficiencies employed in reducing the Ge(Li) detector data.

Isotope	Transition (keV) $E_{xi} \rightarrow E_{xf}$	Transition ^a energy (keV)	Branching ratio	Internal ^b conversion coefficient α	γ detection efficiency ^c $10 \times \epsilon_\gamma$	Ratio ^{a,d} $\epsilon_e/\epsilon_\gamma$
⁷⁰ Ge	1040 \rightarrow g.s.	1040	1	3.2×10^{-4}	0.041	43
⁷⁰ Ge	1216 \rightarrow 1040	176	0.012	0.09	f	
⁷⁰ Ge	1216 \rightarrow g.s.	1216	0.988	∞^e	0.037	47
⁷² Ge	690 \rightarrow g.s.	690	1	$> 20^a$	0.072	24
⁷² Ge	835 \rightarrow 690	145	$< 3 \times 10^{-5}$	0.19	f	
⁷² Ge	835 \rightarrow g.s.	835	1	5.4×10^{-4}	0.056	31
⁷⁴ Ge	596 \rightarrow g.s.	596	1	1.4×10^{-3}	0.090	19
⁷⁴ Ge	1205 \rightarrow 596	609	0.7	1.4×10^{-3}	0.086	20
⁷⁴ Ge	1205 \rightarrow g.s.	1205	0.3	2.2×10^{-4}	0.042	42
⁷⁶ Ge	563 \rightarrow g.s.	563	1	1.6×10^{-3}	0.098	18
⁷⁶ Ge	1123 \rightarrow 563	560	0.7 ^e	1.6×10^{-3}	0.098	18
⁷⁶ Ge	1123 \rightarrow g.s.	1123	0.3 ^e	2.6×10^{-4}	0.040	44

^a Values from Ref. 5.

^b Values refer to *E2* transitions as given in Ref. 30.

^c See text for derivation.

^d ϵ_e assumed 0.175 for all internally converted transitions.

^e Assumed value.

^f Not observed.

procedures employed in determining the cross-section magnitude from the measured γ -ray values. The uncertainties in the absolute cross sections were estimated to range from $\pm 15\%$ for the excitation of the well-defined 595-keV state in ^{74}Ge to as much as $\pm 40\%$ for the cross sections derived from the full energy peaks at 1.038 and 1.207 MeV. These estimates of error are inclusive of uncertainties in full-energy-peak counts, relative detection efficiencies, flux determinations, and reference cross sections. Uncertainties associated with multiple neutron scattering and to the internal conversion coefficient α were not included in the estimates of error. The former were estimated to be less than 5%. The latter were also small since

$$\sigma \propto [\epsilon_\gamma/(\alpha+1) + \epsilon_e\alpha/(\alpha+1)]^{-1} \quad (4)$$

and thus

$$\frac{\delta\sigma}{\sigma} = \left(\frac{\alpha}{\alpha+1}\right) \left[\left(1 - \frac{\epsilon_e}{\epsilon_\gamma}\right) / \left(1 + \alpha \frac{\epsilon_e}{\epsilon_\gamma}\right) \right] \frac{\delta\alpha}{\alpha} = K \frac{\delta\alpha}{\alpha},$$

where ϵ_γ and ϵ_e are the absolute average efficiencies for detection of γ -ray and internal conversion transitions, respectively, generated in the bulk of the detector. In the present work, $|K|$ was typically ≈ 0.02 for transitions proceeding largely by γ -ray emission and considerably less for transitions proceeding primarily by internal conversion. Values of transition parameters and detection efficiencies used in evaluating the relative cross sections are listed in Table II.

The cross sections derived from the 0.835-MeV γ transition in ^{72}Ge (Fig. 7) included a correction of approximately 10% for contamination by the 0.842-MeV transition in ^{27}Al , a consequence of inelastic neutron scattering by the aluminum structural material in the vicinity of the detector. This contribution was estimated from the experimental geometry and the cross sections of neutron scattering³⁶ from both the 0.842- and 1.013-MeV states in ^{27}Al . A small peak attributed to the 1.013-MeV transition in ^{27}Al was observed in a number of spectra. The peak at 1.207 MeV probably consisted of unresolved components from the 1.205-MeV $2+ \rightarrow 0+$ (g.s.) transition in ^{74}Ge and the 1.216-MeV $0+ \rightarrow 0+$ (g.s.) transition in ^{70}Ge . The results for this doublet have been plotted in Fig. 9 as a dummy cross section σ^* which has been normalized such that

$$\sigma^* = 0.59\sigma_{1.216} + 0.41\sigma_{1.205}, \quad (5)$$

where the numerical coefficients shown for the excitation cross sections of the two states have been obtained from the values of Table II and from an assumed 3.3 mm thickness of the Ge(Li) detector.

The cross sections derived from the time-of-flight and

from the γ -ray measurements were in reasonably good agreement. The excitation of the 0.595-MeV state in ^{74}Ge was used for normalizing results obtained with both methods, thus the agreement of Fig. 5 is not significant. The agreement between methods in the observed excitation of the 0.563-MeV state in ^{76}Ge (Fig. 6) is reasonable in view of the low (7.8%) abundance of the isotope. Cross sections for the excitation of the $2+$, 0.835-MeV state in ^{72}Ge obtained with the time-of-flight method are somewhat lower in the incident energy range 1.4–1.5 MeV than those obtained from the γ -ray observations (Fig. 7) but the discrepancy is not outside the combined uncertainties of the two results. Similar comment pertains to the excitation of the $2+$, 1.038-MeV state in ^{70}Ge (Fig. 8). Comparison of absolute cross sections for the excitation of the 0.692-MeV state in ^{72}Ge obtained using the two methods is again not significant due to the normalization procedure described above. No time-of-flight data were available for the excitation of states at $1.2 \gtrsim \text{MeV}$.

The results of statistical Hauser-Feshbach CN calculations based upon the above "best" spherical optical-model parameters are indicated by the solid curves of Figs. 5–9. The excitation energy of the second $2+$ state in both ^{74}Ge and ^{76}Ge was very nearly twice that of the respective first $2+$ states, so that in each case the two γ rays of the cascade were not experimentally resolved. The long-short dashed curves of Figs. 5 and 6 represent the calculated results adjusted for the summing of these cascades and are comparable with the γ -ray experimental results. Results of calculations inclusive of corrections for width fluctuations and correlations ($Q=0$) are indicated by dashed lines in the figures.

IV. DISCUSSION

The results of the present experiments are in general agreement with partial and total cross sections obtained in previous experimental studies of neutron interactions with germanium. Figure 10 compares the elastic and total inelastic cross-section results with the reported total neutron cross sections and with the results of calculations. In the present work, inelastic neutron scattering from ^{73}Ge (abundance $\approx 8\%$) has been neglected. No such processes were observed and calculations indicated that any such contributions would be small ($\lesssim 0.07$ b). The present elastic scattering angular distributions agreed within experimental error with those reported by Cox.¹² The relative cross sections for the $(n, n'\gamma)$ processes in germanium reported by Barry,¹³ if normalized to the present time-of-flight results in the manner described above, are in fair agreement with the values of the present γ -ray studies.

The energy-smoothed measured inelastic cross sections were reasonably described by calculations based upon the Hauser-Feshbach formula³ (see Figs. 5–9). The agreement between these calculations and the

³⁶J. P. Chien and A. Smith, Nucl. Sci. Eng. 26, 500 (1966).

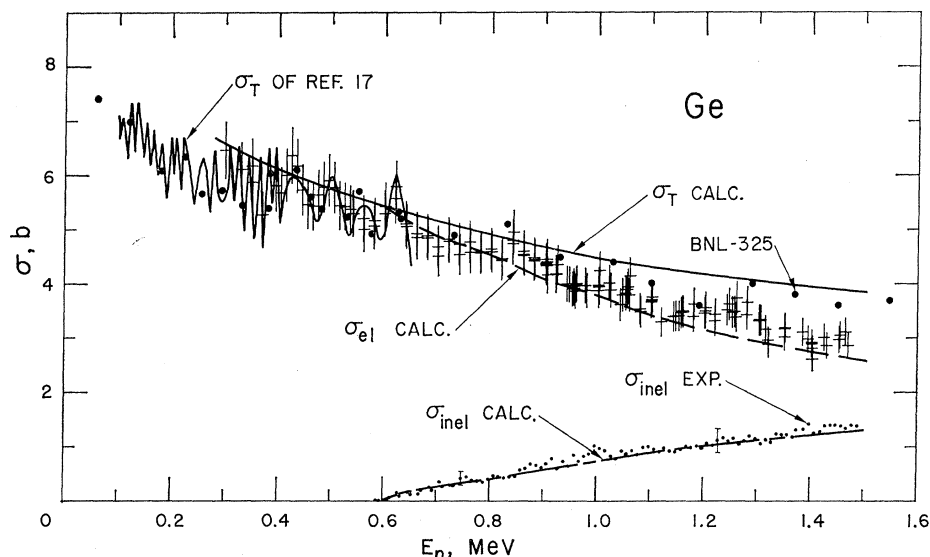


FIG. 10. Neutron cross sections of natural germanium. Crosses denote the experimental σ_{e1} values of Fig. 4 and small dots the measured total inelastic scattering cross sections obtained by summing individual excitation values. Total cross sections of Whalen and Meadows (Ref. 17) (fluctuating curve) and as given in BNL-325 (Ref. 15) (large dots) are shown. Total elastic and total inelastic cross sections calculated from the optical potential of Sec. II and statistical CN theory are also indicated.

excitation of the first states in ^{70}Ge and ^{72}Ge as measured by time-of-flight studies was good. The correspondence between theory and experiment was less satisfactory for the excitation of the 0.595-MeV state in ^{74}Ge . Where discrepancies did exist, the result calculated using the Hauser-Feshbach form was usually smaller than the measured value. The measured total cross sections in the interval 0.1–0.65 MeV¹⁷ and CN level systematics indicated that the CN levels of the germanium isotopes at the energies of the present experiments appreciably overlapped. Thus, the statistical parameter Q of Eq. (3) should approach zero. In that case only the width fluctuation correction is appreciable. When applied, the inelastic results are $\geq 30\%$ below Hauser-Feshbach or experimental values (see dashed curves of Figs. 5–8). Maximum values of $Q=1$ (isolated CN levels) resulted in calculated values 20–30% lower than experiment. The correction factors had only a minor effect on the calculated elastic scattering cross sections.

The theoretical basis of width fluctuation and correlation corrections has been extensively defined⁴ and there has been wide experimental support of such corrections.^{37–43} However, in the germanium mass region the agreement between results of corrected calculations and

experiment has not always been good. Uncorrected Hauser-Feshbach values tended to give a better agreement with the measured inelastic scattering cross section of zinc at 1.5 MeV⁴² and possibly a similar tendency was present in the results of inelastic scattering from selenium reported by Glazkov.⁴⁴

Differences between calculated and measured inelastic cross sections could be attributed to uncertainties in the relevant excited structure. In the present context, this seems unlikely as the low-lying structure of the even isotopes of germanium, well known from Coulomb excitation and other experiments, apparently consists of one- and two-quanta vibrational excitations.⁵ Such structure is strongly influenced by shell configurations.⁴⁵ This influence may be evident in the germanium isotopes where ^{72}Ge is presumed to complete the $p_{1/2}$ neutron subshell and ^{74}Ge is formed by the addition of a pair of neutrons to the $g_{9/2}$ subshell. The splitting of the two-quanta vibrational excitation into 0^+ , 2^+ , and 4^+ states and the magnitudes of the quadrupole deformation parameter β_2 are markedly different for ^{72}Ge and ^{74}Ge .⁴⁶ All of the present calculations are model-dependent and it is known that major shell closures can appreciably effect the choice of potential.^{47,48} Thus it is likely that the simple spherical and mass-independent

³⁷ W. Vonach and A. Smith, Nucl. Phys. **78**, 389 (1966).

³⁸ E. Barnard *et al.*, Nucl. Phys. **A118**, 321 (1968).

³⁹ K. Nishimura *et al.*, Nucl. Phys. **70**, 421 (1965).

⁴⁰ A. Tucker *et al.*, Phys. Rev. **137**, B1181 (1965).

⁴¹ J. Towle *et al.*, *Nuclear Data for Reactors* (International Atomic Energy Agency, Vienna, 1967), Vol. 1.

⁴² S. Mathur *et al.*, Phys. Rev. **160**, 816 (1967).

⁴³ A. Smith *et al.*, Phys. Rev. **135**, B76 (1964).

⁴⁴ N. P. Glazkov, At. Energy (USSR) **15**, 416 (1963).

⁴⁵ A. Bohr and B. R. Mottelson, *Nuclear Spectroscopy*, edited by F. Ajzenberg-Selove (Academic Press Inc., New York, 1960), Part B, pp. 1009–1032.

⁴⁶ P. Stelson and L. Grodzins, Nucl. Data **A1**, 1 (1960).

⁴⁷ W. Vonach *et al.*, Phys. Letters **11**, 331 (1964).

⁴⁸ A. Lane *et al.*, Phys. Rev. Letters **2**, 424 (1959).

potential defined here is an oversimplification taking cognizance of neither shell effects nor possible coupling between various channels. Both effects may change from isotope to isotope. A coupled-channel calculation of the inelastic excitation of the first $2+$ state of ^{74}Ge was carried out using a deformed potential.⁴⁹ The parameters of the spherical well given above were retained with a $\beta_2=0.28$ and a direct well equivalent to the real potential. The results at 1.0 MeV are indicated by the dotted curves of Fig. 2. The calculated inelastic scattering is $\approx 20\%$ greater than that obtained with the Hauser-Feshbach formula and closer to the experimental values. The calculated inelastic angular distribution is slightly nonsymmetric about 90° but not to a degree measurable by the present experiments. The coupled-channel calculation yields total and elastic scattering cross sections that are not particularly descriptive of experiment but such differences are much reduced when the calculated results are corrected for the 36% abundance of ^{74}Ge in the natural element. Thus, a model properly accounting for vibrational effects appreciably improves the agreement between calculated and measured inelastic scattering from ^{74}Ge . Further detailed adjustments of the potential on an isotope by isotope basis accounting for variations due to shell structure and deformation could well lead to calculated inelastic results requiring fluctuation correction factors for good agreement with experiment. Such detailed adjustments were not attempted as the experimental knowledge of elastic scattering from individual isotopes needed for proper definition of the potential was not available.

The elastic and inelastic cross sections observed in these experiments and the reported total cross sections¹⁷ have exhibited a rapid energy variation characterized by a width and a spacing intermediate between that of single-particle and CN resonances. The effect was particularly evident in the inelastic excitation of the 0.692 MeV ($0+$) state in ^{72}Ge where the observed

fluctuations of $\approx 15\%$ exceeded the experimental uncertainties of $\lesssim 10\%$. A number of interpretations of such intermediate structure have been proposed including effects due to resonance width fluctuations in regions of large transmission coefficients^{50,51} and to quasiparticle intermediate resonances.⁵² In the present experimental context, neither the statistical accuracy nor energy resolution of the measurements were felt sufficient to warrant a quantitative comparison of the observed structure and theory.

V. CONCLUSION

The observed elastic and inelastic neutron scattering cross sections of germanium have been reasonably well described by a spherical, mass-independent, optical potential and the Hauser-Feshbach statistical theory. The form of the optical potential employed was consistent with that found applicable in a similar mass-energy region. Modification of the statistical theory to provide corrections for resonance width fluctuations and correlations did not result in improved agreement with experiment. It was qualitatively suggested that discrepancies between the modified CN model calculation and experiment were due to deficiencies in the model and potential in a region of rapidly changing shell structure and in the presence of strong vibrational excitations.

ACKNOWLEDGMENTS

The authors wish to acknowledge the assistance of a number of members of the Reactor Physics Division. We are grateful to Dr. E. Bennett for preparing and making available to us the proportional counter, and to Dr. D. C. Stupegia for making available the Ge(Li) detector. Thanks are also due to W. J. Snow for computations of the γ -ray detection efficiencies of germanium, and to Dr. P. A. Moldauer for helpful discussions.

⁴⁹ C. L. Dunford, Atomics International Report No. NAA-SR-11706, 1966 (unpublished).

⁵⁰ P. A. Moldauer, Phys. Rev. Letters **18**, 249 (1967).

⁵¹ P. A. Moldauer, Argonne National Laboratory Report No. ANL-7467, 1968 (unpublished).

⁵² H. Feshbach *et al.*, Ann. Phys. (N.Y.) **41**, 230 (1967).